Communications in Physics, Vol. 36, No. 1 (2026), pp. 47-56
DOI: https://doi.org/10.15625/0868-3166/23580

Machine learning–assisted ECNLE theory for predicting dynamical properties of FeCoCrMoCBTm metallic glass

Ngo T. Que[1,‡], **Anh D. Phan**[1,2,†], **Do T. Nga**[3] **and Tran Van Huynh**[4]

[1]*Phenikaa Institute for Advanced Study, Phenikaa University, Hanoi 12116, Vietnam*

[2]*Faculty of Materials Science and Engineering, Phenikaa University, Hanoi 12116, Vietnam*

[3]*Institute of Physics, Vietnam Academy of Science and Technology, 10 Dao Tan, Giang Vo, Hanoi 11108, Vietnam*

[4]*Department of Basic Sciences and Foreign Languages, University of Fire, 243 Khuat Duy Tien, Hanoi 120602, Vietnam*

E-mail: [†]anh.phanduc@phenikaa-uni.edu.vn; [‡]que.ngothi@phenikaa-uni.edu.vn

Received 4 October 2025
Accepted for publication 23 January 2026
Published 5 March 2026

Abstract. *In this work, we present an integrated modeling framework that combines machine learning and the elastically collective nonlinear langevin equation (ECNLE) theory to investigate the glass transition dynamics of metallic glass systems. We focus on the $Fe_{42}Co_6Cr_{15}Mo_{14}C_xB_{21-x}Tm_2$ alloy family. The glass transition temperatures (T_g) of this alloy family are predicted using machine learning models trained on experimental datasets. These machine learning-predicted-T_g values are then used as input to the elastically collective nonlinear langevin equation theory to compute the temperature dependence of structural relaxation times, dynamic fragility, and diffusion coefficients. Our predictions of T_g and dynamic fragility quantitatively agree with the experimental data. This shows that the combined machine learning-elastically collective nonlinear langevin equation approach provides a practical and scalable tool for characterizing the relaxation behavior and diffusion dynamics metallic glasses when experimental data remain limited.*

Keywords: metallics glasses; relaxation time; diffusion; machine learning.

Classification numbers: 64.70.P; 61.43.Fs; 66.30.-h.

1. Introduction

Metallic glasses (MGs) are a unique class of amorphous alloys that are characterized by the absence of long-range crystalline order yet exhibit outstanding physical and mechanical properties, such as high strength, excellent corrosion resistance, and unique magnetic and thermal behaviors

[1, 2]. These exceptional characteristics have attracted considerable attention in both fundamental research and technological applications, including aerospace, biomedical devices, and electronic materials [1, 2]. Despite their promising potential, the design and optimization of MGs remain challenging due to their compositional complexity and the intricate nature of their thermodynamic and kinetic stability.

A key parameter governing the stability and dynamics of MGs is the glass transition temperature. The T_g defines the transition from a rigid glassy state to a supercooled liquid, thereby influencing important properties such as thermal stability, mechanical performance, and glass-forming ability [3, 4]. Accurate determination of T_g is thus essential for both theoretical understanding and practical design of MGs. However, experimental measurements of T_g often require extensive effort and resources. Techniques such as differential scanning calorimetry and broadband dielectric spectroscopy are time-consuming, and the exploration of large compositional spaces in multi-component alloys is particularly resource-intensive [1, 2].In addition, the available experimental data are sometimes limited or inconsistent, which further constrains their use for developing reliable predictive models of MG properties. Molecular dynamics (MD) simulations offer an alternative method for estimating T_g [5]. However, they require suitable force fields, which are often not available for complex multi-component systems. Additionally, there is a significant discrepancy in quenching time scales between simulations and experiments. While experimental data is typically obtained under standardized cooling rates of 10–20 K/min, MD simulations use much faster cooling rates of around 1 K/ps. Density functional theory [6] also has limitations as it is restricted to 0 K calculations and cannot capture glass transition behavior.

Meanwhile, machine learning has provided new opportunities to overcome these limitations by efficiently and accurately predicting material properties directly from composition. Machine learning (ML) methods have already been successfully applied to predict a wide range of MG properties, such as glass-forming ability, elastic moduli, and crystallization temperatures [7–10]. In particular, ML-based models for predicting T_g offer a promising pathway to accelerate the design of new MGs while minimizing experimental effort [11].

As illustrated in Fig. 1, MD simulations is the relaxation times accessible less than 10^5 ps, while the experimental timescale of glass-forming systems span much longer timescales ranging from milliseconds to hundreds of seconds. This means that the slow structural relaxation dynamics near and below T_g cannot be directly accessed by MD simulations. To bridge this timescale gap, the elastically collective nonlinear langevin equation (ECNLE) theory has been developed to describe the temperature and pressure dependence of structural relaxation in various glass-forming systems [12–23]. A wide range of systems theoretically described by the ECNLE theory include thermal liquids [17, 18], polymers [13], colloidal suspensions [16, 21], metallic glasses [20], amorphous pharmaceuticals [13–15], and nanocomposites [5, 19]. It captures the interplay between local cage-scale dynamics and long-range collective elastic effects to provide quantitative understandings of key dynamical quantities including structural relaxation times, diffusion coefficients, and dynamic shear moduli. The ECNLE theory only requires the glass transition temperature as an input parameter. This means that by combining ML-predicted T_g values with the ECNLE theory, the data-driven approach can be exploited to investigate the relaxation behavior of metallic glasses when experimental T_g's are not available.

In this work, we focus on the $Fe_{42}Co_6Cr_{15}Mo_{14}C_xB_{21-x}Tm_2$ ($x = 9, 11, 13, 15, 17$) alloy family, a representative Fe-based metallic glass system. Fe-based MGs are of particular interest

due to their cost-effectiveness, wide applicability, and sensitivity to compositional tuning, especially with respect to the C/B ratio [24, 25]. To the best of our knowledge, these materials have not been systematically investigated through theoretical or computational approaches. To advance the understanding of this alloy family, our study addresses the following several questions: (1) Can machine learning models accurately predict the glass transition temperature of these alloys? (2) Can the ECNLE theory provide reliable quantitative insights into their dynamical properties? (3) What is the effect of carbon doping on the glass transition and dynamical behavior of these materials? Answering these questions not only deepens the understanding of Fe-based MGs when experimental data are limited but also provides further validation of the ECNLE framework in predicting the structural relaxation time.

2. Theoretical background

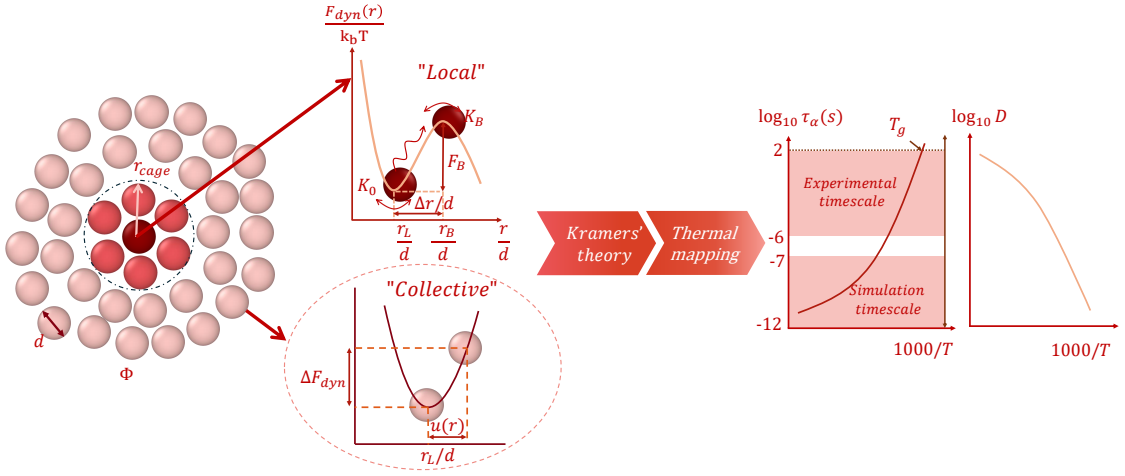

Fig. 1. (Color online) Workflow of the ECNLE theory for the structural relaxation time, diffusion process.

In the ECNLE theory [12–23] amorphous systems describes glass-forming liquids as a hard-sphere fluid characterized by the particle diameter, d, density number, ρ, and the volume fraction, $\Phi = \rho\pi d^3/6$ as Fig. 1. The radial distribution function, $g(r)$, and static structure factor, $S(q)$ where q is the wavevector, are determined using the Percus-Yevick integral equation theory. The dynamics of a tagged particle is governed by interactions with its nearest neighbors and cooperative motion of the surrounding fluid. The local dynamics, describing the tagged particle's motion within its cage, is quantified by the dynamic free energy, $F_{\rm dyn}(r)$, expressed as the sum of two contributions $F_{\rm dyn}(r) = F_{\rm ideal}(r) + F_{\rm caging}(r)$. Here,

$$\frac{F_{\rm dyn}(r)}{k_BT} = -3\ln\left(\frac{r}{d}\right) - \int_0^\infty \frac{q^2d^3[S(q)-1]^2}{12\pi\Phi[1+S(q)]}\exp\left[-\frac{q^2r^2(1+S(q))}{6S(q)}\right]dq, \tag{1}$$

where k_B is the Boltzmann constant, T is the ambient temperature, r is the displacement. The first term on the right-hand side of Eq. (1) represents the ideal fluid-like contribution, whereas the second term captures the caging constraints arising from interactions with neighboring particles.

$F_{\text{ideal}(r)} = -3k_BT\ln(r/d)$ represents the free energy of the delocalized (ideal fluid) state, while $F_{\text{caging}}(r)$ captures the localized state reflecting the influence of density and structural order. Detailed analyses of $F_{\text{caging}}(r)$, employing the volume fraction and $S(q)$, can be found in previous studies [12–23].

The dynamic free energy $F_{\text{dyn}}(r)$ provides fundamental information about local particle dynamics. In dilute solutions ($\Phi < 0.43$), $F_{\text{dyn}}(r)$ decreases monotonically with increasing r, indicating that fluid particles can diffuse without significant kinetic constraints [21, 22]. At sufficiently high densities ($\Phi > 0.43$), the free volume is reduced and a insighfull emerges in $F_{\text{dyn}}(r)$, leading to the dynamic confinement of a tagged particle within an intermolecular cage formed by its neighbors [21, 22]. The cage radius, r_{cage}, is determined by the first minimum of the radial distribution function $g(r)$. In this regime, the onset of transient localization occurs as a barrier develops in $F_{\text{dyn}}(r)$. From the free energy profile, the key length and energy scales of local dynamics can be quantified. The local minimum of $F_{\text{dyn}}(r)$ defines the localization length r_L, while the barrier position is denoted by r_B. The jump distance is then given by $\Delta r = r_{\text{B}} - r_{\text{L}}$ and $F_{\text{B}} = F_{\text{dyn}}(r_{\text{B}}) - F_{\text{dyn}}(r_{\text{L}})$, respectively. In addition, we calculate the harmonic curvatures at r_{L} and r_{B} as $K_0 = \left|\dfrac{\partial^2 F_{\text{dyn}}(r)}{\partial r^2}\right|_{r=r_{\text{L}}}$ and $K_{\text{B}} = \left|\dfrac{\partial^2 F_{\text{dyn}}(r)}{\partial r^2}\right|_{r=r_{\text{B}}}$, respectively. K_0 represents the effective spring constant at the localization length, K_B is the absolute curvature at the barrier position.

In many amorphous materials [12–18], cage escape requires cooperative rearrangements of neighboring and surrounding particles, where collective motions are strongly coupled to local dynamics. In contrast, for metallic glasses, the influence of collective motion on the glass transition is generally regarded as negligible, with local dynamics being the dominant factor [19, 20]. Therefore, considering only the local barrier within Kramer's theory offers a reasonable approximation for evaluating the structural relaxation time [12–23]

$$\frac{\tau_\alpha}{\tau_s} = 1 + \frac{2\pi}{\sqrt{K_0 K_{\text{B}}}} \frac{k_{\text{B}}T}{d^2} \exp\left(\frac{F_{\text{B}}}{k_{\text{B}}T}\right), \tag{2}$$

where τ_s is a short-time scale defined elsewhere [12–23]. Equation (2) provides the density dependence of the structural relaxation time. In metallic glasses, nearest-neighbor intereactions play an important role in the glass transition and contribution of the collective dynamics to this phenomenon can be ignored. For quantitative comparison with experimental data, we use the density-to-temperature conversion constructed using the thermal expansion process [12–23]

$$T = T_g + \frac{\Phi_g - \Phi}{\beta \Phi_0}, \tag{3}$$

where T_g is the glass transition temperature ($\tau_\alpha(T_g) = 100\,\text{s}$) given by experiments [26, 27] or ML prediction [11], $\Phi_0 \approx 0.50$ is a characteristic volume fraction, $\Phi_g \approx 0.6714$ is the volume fraction at $\tau_\alpha(\Phi_g) = 100$ s for metallic glasses, and $\beta \approx 12 \times 10^{-4}\,\text{K}^{-1}$ is an effective thermal expansion coefficient [12–23].

From the temperature dependence of τ_α, we can calculate the dynamic fragility, which is [23]

$$m = \left.\frac{\partial \log_{10}\tau_\alpha}{\partial(T_g/T)}\right|_{T=T_g}. \tag{4}$$

The fragility index provides a useful criterion to classify amorphous materials into three categories including strong ($m \leq 30$), intermediate ($30 < m < 100$), and fragile ($m \geq 100$) [23].

The relationship between the diffusion coefficient (D) and the structural relaxation time is described by:

$$D(T) = \frac{\langle \Delta r \rangle^2}{6\,\tau_\alpha(T)}. \tag{5}$$

In several previous studies [19,20], diffusion coefficients calculated using the ECNLE theory have shown good agreement with experimental measurements for various glass-forming systems.

To evaluate the performance of the employed machine learning models, we used three statistical metrics including the coefficient of determination (R^2), the root mean square error (RMSE), and the mean absolute error (MAE). These metrics are defined as follows

$$R^2 = 1 - \frac{\sum_{i=1}^{n}(y_i - \hat{y}_i)^2}{\sum_{i=1}^{n}(y_i - \bar{y})^2}, \tag{6}$$

$$RMSE = \sqrt{\frac{1}{n}\sum_{i=1}^{n}(y_i - \hat{y}_i)^2}, \tag{7}$$

$$MAE = \frac{1}{n}\sum_{i=1}^{n}|y_i - \hat{y}_i|, \tag{8}$$

where y_i and $\hat{y}_i$ denote the experimental and predicted values, respectively, $\bar{y}$ is the mean of the experimental values, and n is the total number of data points.

3. Results and discussion

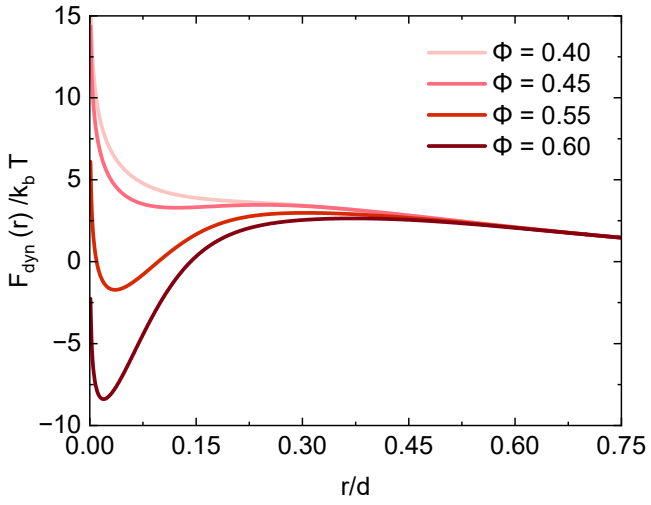

Fig. 2. (Color online) Dynamic free energy as a function of displacement at different volumn fractions Φ.

Figure 2 shows the dependence of the dynamic free energy ($F_{\rm dyn}$) on displacement (r) at different packing fractions $\Phi = 0.40, 0.45, 0.55$, and 0.60. As the volume fraction increases, the shape of the $F_{\rm dyn}$ curves changes significantly. At $\Phi = 0.40$ and $\Phi = 0.45$, the dynamic free energy exhibits a shallow minimum and a low energy barrier. This indicates that the system still allows for considerable structural rearrangements and retains relatively loose dynamics. When Φ increases from 0.55 to 0.60, the energy barrier becomes deeper. It means stronger constraints on particle motion and enhanced stability of the dynamic glassy state. This also signifies stronger caging effects and the tendency toward dynamical arrest as the system approaches the glass transition. These results reveal that with increasing packing fraction, the dynamic free energy evolves from a nearly flat profile to one with a distinct barrier and fundamentally changes from liquid-like dynamics to glassy behavior. This is in agreement with the predictions of the ECNLE theory.

Table 1. The glass transition temperatures in Kelvin predicted from our ExtraTrees Regression model and their corresponding experimental values in Ref. [26].

x	$T_{g,exp}(K)$	$T_{g,ML}(K)$
9	876	876
11	872	872
13	871	871
15	850	855.5
17	845	845

In our previous work [11], we trained machine learning models using a dataset consisting of 715 experimentally measured data points. In order to improve the generalization ability of the model and expand its applicability to a wider range of metallic glass compositions, we expanded the dataset to a total of 921 experimental data points by adding data from the literature. Each alloy composition in the dataset was represented by a set of 45 elemental features, which is an increase of three elemental features compared to [11] since we have more alloys. To validate our calculations, we randomly divided the dataset into 80% for training and 20% for testing. This split ensures that calculations on the test set are completely independent from those on the training data. We then used a grid search procedure [28] to optimize the hyperparameters of the ExtraTrees regression model..The optimized model was trained on the training subset and evaluated on the held-out test set. Numerical results on the testing dataset are $MAE = 7.73$ K, $RMSE = 12.03$ K, and $R^2 = 99.37\%$. To further evaluate predictive performance of our model, we carried out a 5-fold cross-validation on the full dataset [29]. The averaged results are $R^2 = 98.8\%$, $RMSE = 16.15$ K, and $MAE = 9.73$ K. This finding indicates that the model's performance is consistent across different data partitions.

After training and validation, the optimized model was employed to predict the glass transition temperatures of the alloys $Fe_{42}Co_6Cr_{15}Mo_{14}C_xB_{21-x}Tm_2$ with $x = 9$, 11, 13, 15, and 17. Note that the data of $Fe_{42}Co_6Cr_{15}Mo_{14}C_xB_{21-x}Tm_2$ is in our dataset but training and testing data are randomly split. This treatment ensures the model has relatively high accuracy due to be trained on large dataset meanwhile contains sufficient generalization. The randomness of splitting dataset allows us to avoid bias when evaluating the model. As shown in Table 1, the predicted T_g values are in reasonable agreement with the corresponding experimental data for $x = 9, 11, 13$, and 17

with a deviation of approximately 5.5 K observed at $x = 15$. In our dataset, the carbon concentration is primarily distributed within the range of 0–17. Therefore, the predictions for alloys with $x \leq 17$ are reliable since the calculating interval is within the compositional range of the dataset. Increasing the carbon content can lead to predictions outside the range of the training data and enhance uncertainty. However, we expect that changing x from 17 to 21 is so small that predictive results are still reliable. This is an open question for future simulation and experimental study.

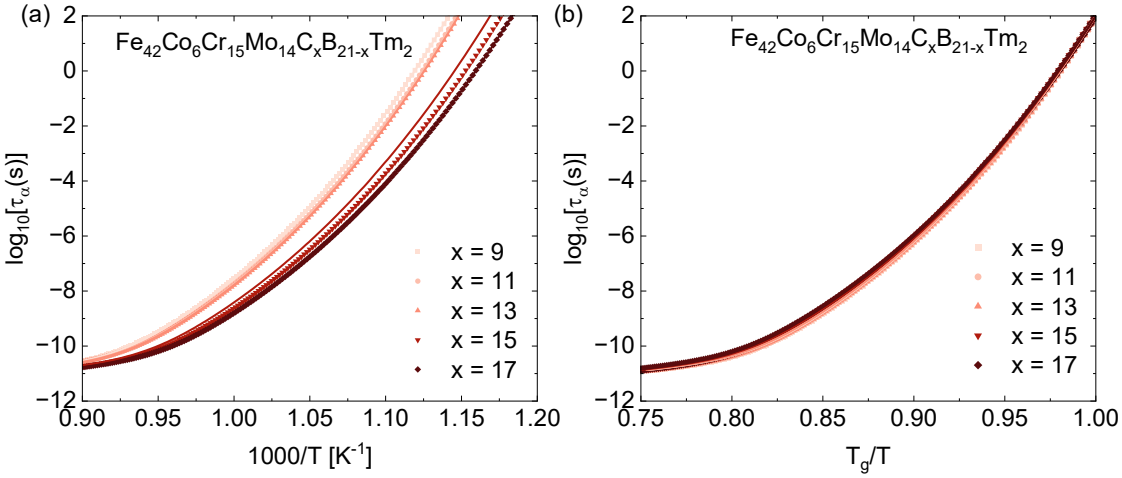

Fig. 3. (Color online) The logarithm of the structural relaxation time (in seconds) for the $Fe_{42}Co_6Cr_{15}Mo_{14}C_xB_{21-x}Tm_2$ (x = 9, 11, 13, 15 and 17 at.%) metallic glass as a function of (a) $1000/T$ and (b) T_g/T calculated using the T_gs values from ML predicted (solid curve) and T_gs values experimental (data points).

The predicted T_g values from our ML model were used as input in Eqs. (2) and (3) to predict the temperature dependent structural relaxation time. The results in Fig. 3 indicate a strong consistency between ECNLE calculations based on either experimental or ML-predicted T_g. As the C concentration increases, τ_α decreases, which signifies enhanced atomic mobility. This behavior arises because, at a fixed temperature, the increases of C lowers T_g, thereby promoting faster relaxation dynamics. Although we do not have experimental data for structrural relaxation time to compare with our theoretical numerical results, it is possible to evalute the accuracy of prediction τ_α via the fragility calculation obtained from Fig. 3(b) using Eq. (4)

Given the quantitative agreement between the ML-predicted and experimental T_g values, the fragility values calculated using Eq. (4) are also expected to be very similar. Table 2 presents the dynamic fragility computed using ECNLE theory with T_g values from ML predictions, compared with experimental data. The results indicate good consistency with experimental estimates for $x = 9, 11$, and 13, whereas larger deviations are observed for higher C contents ($x = 15$ and 17). This outcome suggests that the method is more accurate in the low C concentration regime, whereas additional refinements may be required to capture the fragility of alloys with higher C/B ratios.

Based on this, we used Eq. (5) to calculate the diffusion coefficient as a function of 1000/T. As shown in Fig. 4, the diffusion coefficient exhibits a strong dependence on temperature. The

Table 2. The dynamic fragility computed using the ECNLE theory with T_g values from ML predictions (Table 1) and experimental data from Ref. [26].

x	m_{ML}	m_{expt}
9	50.8	55
11	50.6	50
13	50	47
15	48.86	41
17	48.75	80

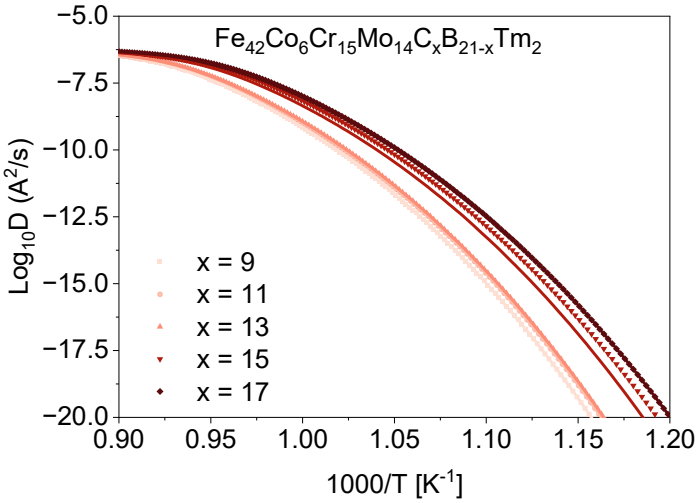

Fig. 4. (Color online) The self-diffusion coefficient for $Fe_{42}Co_6Cr_{15}Mo_{14}C_xB_{21-x}Tm_2$ (x = 9, 11, 13, 15 and 17 at%) metallic glass as a function of $1000/T$ calculated using the T_gs values from ML predicted (solid curve) and T_gs values experimental (data points).

alloy lattice constant $d = 3.13$ Å, obtained from Vegard's law [30], was used to calculate the diffusion coefficient. Since d remains nearly unchanged across different values of x, the variation in carbon and boron concentration has little influence on the results. The diffusion coefficient decreases rapidly with increasing $1000/T$, indicating that atomic mobility is significantly suppressed at lower temperatures. Moreover, the curves corresponding to $x = 9$, 11, 13, 15, and 17 nearly overlap, suggesting that the diffusion process in these metallic glasses is primarily governed by thermal activation energy rather than by minor compositional changes.

4. Conclusion

In conclusion, we have presented a combined machine learning - ECNLE framework to study the glass transition dynamics of $Fe_{42}Co_6Cr_{15}Mo_{14}C_xB_{21-x}Tm_2$ metallic glasses. The ML model accurately predicted T_g, which served as reliable input for ECNLE to compute relaxation

times and diffusion coefficients. In addition, the approach yields fragility values that are consistent with experimental data for low carbon contents, while larger deviations appear at higher C concentrations, thus offering further insights into the composition–dependent dynamic properties of metallic glasses. The ML - ECNLE framework provides an effective and scalable tool for predicting relaxation and diffusion behavior in metallic glasses, especially when experimental data are limited.

Acknowledgments

This research was funded by the Vietnam National Foundation for Science and Technology Development (NAFOSTED) under Grant No. 103.01-2023.62.

Conflicts of interest

The authors have no conflicts to disclose.

Data availability

The data that support the findings of this study are available from the corresponding author upon reasonable request.

References

[1] W. H. Wang, *The elastic properties, elastic models and elastic perspectives of metallic glasses*, Prog. Mater. Sci. **57** (2012) 487.
[2] W. H. Wang, *Dynamic relaxations and relaxation-property relationships in metallic glasses*, Prog. Mater. Sci. **106** (2019) 100561.
[3] Z. P. Lu and C. T. Liu, *A new glass-forming ability criterion for bulk metallic glasses*, Acta Mater. **50** (2002) 3501.
[4] A. Inoue, *Stabilization of metallic supercooled liquid and bulk amorphous alloys*, Acta Mater. **48** (2000) 279.
[5] A. D. Phan, D. T. Nga, N. T. Que, H. Peng, T. Norhourmour and L. M. Tu, *A multiscale approach to structural relaxation and diffusion in metallic glasses*, Comput. Mater. Sci. **251** (2025) 113759.
[6] E. Engel and R. M. Dreizler, *Density Functional Theory: An Advanced Course*. Springer, 2013.
[7] A. Ghorbani, A. Askari, M. Malekan and M. Nili-Ahmadabadi, *Thermodynamically-guided machine learning modelling for predicting the glass-forming ability of bulk metallic glasses*, Sci. Rep. **12** (2022) 11754.
[8] J. Xiong, S. Q. Shi and T. Y. Zhang, *Machine learning prediction of glass-forming ability in bulk metallic glasse*, Comput. Mater. Sci. **192** (2021) 110362.
[9] J. Zhang, M. Zhao, C. Zhong, J. Liu and K. Hu, *Data-driven machine learning prediction of glass transition temperature and the glass-forming ability of metallic glasses*, Nanoscale **15** (2023) 18511.
[10] N. Amigo, S. Palominos and F. J. Valencia, *Machine learning modeling for the prediction of plastic properties in metallic glasses*, Sci. Rep. **13** (2023) 348.
[11] N. T. Que, A. D. Phan, T. Tran, P. T. Huy, M. X. Trang and T. V. Luong, *Machine learning-integrated modeling of thermal properties and relaxation dynamics in metallic glasses*, Mater. Today Commun. **45** (2025) 112287.
[12] A. D. Phan, A. Jedrzejowska, M. Paluch and K. Wakabayashi, *Theoretical and experimental study of compression effects on structural relaxation of glass-forming liquids*, ACS Omega **5** (2020) 11035.
[13] A. D. Phan, K. Wakabayashi, M. Paluch and V. D. Lam, *Effects of cooling rate on structural relaxation in amorphous drugs: elastically collective nonlinear langevin equation theory and machine learning study*, RSC Adv. **9** (2019) 40214.
[14] A. D. Phan and K. Wakabayashi, *Theory of structural and secondary relaxation in amorphous drugs under compression*, Pharmaceutics **12** (2020) 177.
[15] A. D. Phan, J. Knapik-Kowalczuk, M. Paluch, T. X. Hoang and K. Wakabayashi, *Theoretical model for the structural relaxation time in coamorphous drugs*, Mol. Pharmaceutics **16** (2019) 2992.

[16] S. Mirigian and K. S. Schweizer, *Elastically cooperative activated barrier hopping theory of relaxation in viscous fluids. i. genaral formulation and application to hard sphere fluids*, J. Chem. Phys. **140** (2014) 194506.
[17] S. Mirigian and K. S. Schweizer, *Unified theory of activated relaxation in liquids over 14 decades in time*, J. Phys. Chem. Lett. **4** (2013) 3648.
[18] S. Mirigian and K. S. Schweizer, *Elastically cooperative activated barrier hopping theory of relaxation in viscous fluids. II. Thermal liquids*, J. Chem. Phys. **140** (2014) 194507.
[19] A. D. Phan, A. Zaccone, V. D. Lam and K. Wakabayashi, *Theory of pressure-induced rejuvenation and strain hardening in metallic glasses*, Phys. Rev. Lett. **126** (2021) 025502.
[20] N. K. Ngan, A. D. Phan and A. Zaccone, *Impact of high pressure on reversible structural relaxation of metallic glass*, Phys. Status Solidi RRL **15** (2021) 2100235.
[21] K. S. Schweizer and E. J. Saltzman, *Activated hopping and the glass transition*, J. Chem. Phys. **119** (2003) 1181.
[22] K. S. Schweizer, *Derivation of a microscopic theory of barriers and activated hopping transport in glassy liquids and suspensions*, The Journal of chemical physics **123** (2005) 244501.
[23] K. Grzybowska, S. Capaccioli and M. Paluch, *Recent developments in the experimental investigations of relaxations in pharmaceuticals by dielectric techniques at ambient and elevated pressure*, Adv. Drug Deliv. Rev. **100** (2016) 158.
[24] H. X. Li, Z. C. Lu, S. L. Wang, Y. Wu and Z. P. Lu, *Fe-based bulk metallic glasses: Glass formation, fabrication, properties and applications*, Prog. Mater. Sci. **103** (2019) 235.
[25] Z. B. Jiao, H. X. Li, J. E. Gao, Y. Wu and Z. P. Lu, *Effects of alloying elements on glass formation, mechanical and soft-magnetic properties of fe-based metallic glasses*, Intermetallics **19** (2011) 1502.
[26] Q. Wang, X. Yang, Z. Cui, L. Xue, L. Shao, Q. Luo *et al.*, *Effects of c/b ratio on glass-forming ability and low-temperature magnetic behavior of fecocrmocbtm metallic glass*, J. Alloys Compd. **864** (2021) 158211.
[27] B. Schmidtke, M. Hofmann, A. Lichtinger and E. A. Rössler, *Temperature dependence of the segmental relaxation time of polymers revisited*, Macromolecules **48** (2015) 3005.
[28] J. Bergstra and Y. Bengio, *Random search for hyper-parameter optimization*, J. Mach. Learn. Res. **13** (2012) 281.
[29] I. K. Nti, O. Nyarko-Boateng and J. Aning, *Performance of machine learning algorithms with different k values in k-fold cross-validation*, Int. J. Inf. Technol. Comput. Sci. **13** (2021) 61.
[30] K. T. Jacob, S. Raj and L. Rannesh, *Vegard's law: a fundamental relation or an approximation?*, Int. J. Mater. Res. **98** (2007) 776.